Applicability of an Ionic Liquid Electrolyte to a Phosphorus-Doped Silicon Negative Electrode for Lithium-Ion Batteries

Shuhei Yodoya[a,c], Yasuhiro Domi[b,c], Hiroyuki Usui[b,c], and Hiroki Sakaguchi[b,c,*]

We investigated the applicability of an ionic liquid electrolyte to a phosphorus-doped Si (P-doped Si) electrode to improve the performance and safety of the lithium-ion battery. The electrode exhibited excellent cycling performance with a discharge capacity of 1000 mA h g^{-1} over 1400 cycles in the ionic liquid electrolyte, whereas the capacity decayed at the 170th cycle in the organic electrolyte. The lithiation/delithiation reaction of P-doped Si occurred a localized region in the organic electrolyte, which generated a high stress and large strain. The strain accumulated under repeated charge-discharge cycling, leading to severe electrode disintegration. In contrast, the reaction of P-doped Si proceeded uniformly in the ionic liquid electrolyte, which suppressed the electrode disintegration. The P-doped Si electrode also showed good rate performance in the ionic liquid electrolyte; a discharge capacity of 1000 mA h g^{-1} was retained at 10 *C*.

The lithium-ion battery (LIB) has been widely used in portable devices because of its high energy density. LIBs with higher energy density and longer cycle life have been demanded for applications such as electric vehicles and large-scale energy storage for utilizing renewables. Si is a promising candidate negative electrode material for next-generation LIBs because of its high theoretical capacity (3600 mA h g^{-1}) [1,2]. However, the capacity of the Si electrode rapidly fades, which is mainly caused by a significant volume change in Si during Li insertion/extraction. The volume expansion of Si generates a high stress and large strain in active materials, and the strain accumulates under repeated charge-discharge cycling, which causes pulverization and cracking of Si [3,4]. In addition, Si has other disadvantages, including poor electrical conductivity and a low Li^+ diffusion coefficient [5-7]. Doping with impurities has been attempted to improve the chemical properties of negative electrode materials [8]. For example, Sun *et al.* reported that $CuCo_2S_4$@N/S-doped graphene composite electrodes showed good LIB anode performance [9]. We also revealed that P-doping with a very low concentration of approximately 100 ppm helped to dramatically improve the electrochemical performance of Si negative electrodes, which is attributed to suppression of the phase transition from crystalline-Si (*c*-Si) to crystalline-$Li_{15}Si_4$ by P doping into Si rather than an increase in electrical conductivity [10].

[a] S. Yodoya
Department of Engineering, Graduate School of Sustainability Science,Tottori University
4-101 Minami, Koyama-cho, Tottori 680-8552, Japan
[b] Dr. Y. Domi, Dr. H. Usui, and Prof. H. Sakaguchi*
Department of Chemistry and Biotechnology, Graduate School of Engineering, Tottori University
4-101 Minami, Koyama-cho, Tottori 680-8552, Japan
E-mail*: sakaguch@chem.tottori-u.ac.jp
[c] S. Yodoya, Dr. Y. Domi, Dr. H. Usui, and Prof. H. Sakaguchi
Center for Research on Green Sustainable Chemistry, Tottori University
4-101 Minami, Koyama-cho, Tottori 680-8552, Japan

Supporting information for this article is given via a link at the end of the document.

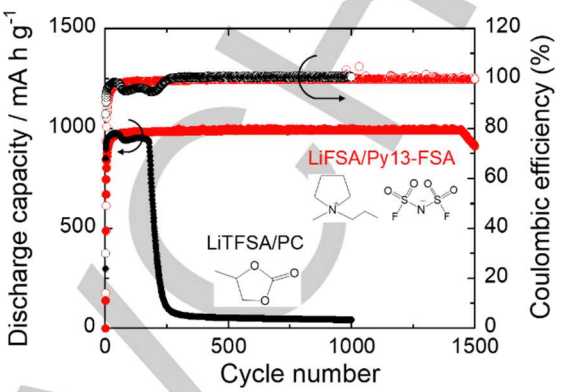

Figure 1. Cycling performance and Coulombic efficiency of P-doped Si electrodes in 1 M LiTFSA/PC and LiFSA/Py13-FSA under a charge capacity limit of 1000 mA h g^{-1} at 0.4 *C* (1st cycle: 0.1 *C*).

Ionic liquids have received much attention as alternatives to flammable organic electrolytes consisting of carbonate-based solvents because of their physicochemical properties, wide electrochemical windows, and high thermal stability. We have investigated the applicability of ionic liquid electrolytes to Si-based electrodes [11-15]. As a result, the cells showed not only high safety but also excellent electrochemical performance in certain ionic liquid electrolytes. In this study, to improve the electrochemical performance and safety of the P-doped Si electrode, we investigated the applicability of an ionic liquid electrolyte to the electrode. In addition, we attempted to elucidate the reaction behavior of the electrode in the ionic liquid electrolyte.

Fig. S1 shows XRD patterns of P-doped Si powders. All peaks were attributed to Si, which is the active material, as shown in Fig. S1a. We confirmed that some of the Si atoms are replaced by P atoms and that P-doped Si is a substitutional solid solution because the peak attributed to Si (1 1 1) shifts to a higher angle after P doping (Fig. S1b). Fig. 1 shows the cycling performance and Coulombic efficiency (CE) of the P-doped Si electrode in an organic electrolyte (LiTFSA/PC) and an ionic liquid electrolyte (LiFSA/Py13-FSA) under a constant charge capacity of 1000 mA h g^{-1}. A typical reaction between Si and Li was observed from the charge-discharge curve and differential capacity vs. potential (d*Q*/d*V*) curves (Fig. S2) [1,2]. The electrode retained a discharge capacity of 1000 mA h g^{-1} only up to 170 cycles in the organic electrolyte, whereas it showed an excellent cycle life with a capacity over 1400 cycles in the ionic liquid electrolyte, which is much superior to the Si-alone electrode (Fig. S3). The CE of the electrode was low in the initial 10 cycles regardless of the electrolyte, which indicates that decomposition of the electrolyte occurred (Fig. S2). A drop in the CE was observed approximately the 60th cycle in the organic electrolyte, which was mainly caused by electrode disintegration and by electrolyte decomposition at a new surface. In contrast, no decrease in the CE was observed in the ionic liquid electrolyte, indicating no electrode disintegration.

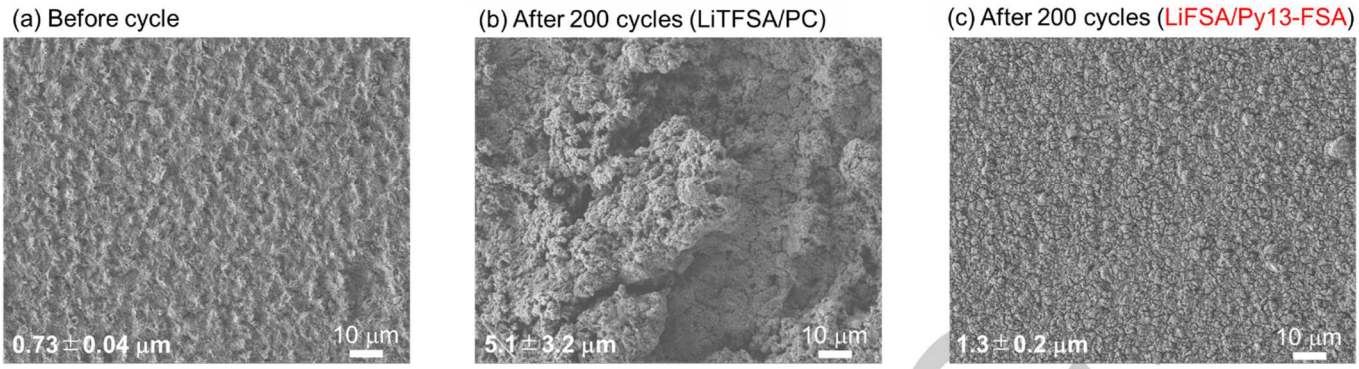

Figure 2. FE-SEM images of P-doped Si electrodes (a) before and (b and c) after 200 cycles. The electrodes were cycled in (b) LiTFSA/PC or (c) LiFSA/Py13-FSA under a charge capacity limit of 1000 mA h g^{-1}. The surface roughness is shown in the bottom left of the images.

To reveal the reasons for the difference in the cycling performance of the P-doped Si electrode in the organic and ionic liquid electrolytes, we evaluated the surface morphology by field emission scanning electron microscopy (FE-SEM). Fig. 2 shows an FE-SEM image of the electrode surface before cycling and after the 200th cycle. The surface roughness calculated by confocal laser scanning microscopy is also shown in the bottom left of the image. Although the surface before cycling was relatively flat, it became clearly rough in the organic electrolyte, and the roughness was obviously larger than that before cycling, which indicates electrode disintegration. In contrast, the surface was flat in the ionic liquid electrolyte, and its roughness was small (before cycle: 0.7±0.04 μm, organic electrolyte: 5.1±3.2 μm, ionic liquid electrolyte: 1.3±0.2 μm).

To clarify the mechanism of electrode disintegration, we investigated the distribution of *c*-Si and amorphous Si (*a*-Si) on the electrode after charge-discharge cycling by Raman mapping analysis (Fig. 3) [16]. The spot diameter of Raman spectroscopy is 710 nm. The red-colored region indicates the presence of crystalline Si, which is Si that is unreacted with Li, and other colored regions indicate Si that has reacted with Li. In the organic electrolyte, *c*-Si corresponds to the red color in the image and is unevenly distributed on the electrode surface (Fig. 3a), which indicates that alloying-dealloying reactions of P-doped Si with Li proceed inhomogeneously. PC-based electrolytes are decomposed to form surface films with uneven thicknesses on the electrodes [17]. Li^+ should be preferentially stored within the P-doped Si through a thinner area of the surface film, where stress is locally generated and strain is accumulated. Therefore, in the organic electrolyte, electrode disintegration should occur at a relatively early stage. In contrast, domains of Si that partially lost their crystallinity, corresponding to the green color in the image, were homogeneously distributed over the electrode surface in the ionic liquid electrode (Fig. 3b). This result is because the surface film derived from the ionic liquid electrolyte is thinner and more stable than that from the organic electrolyte [18]. Therefore, the ionic liquid electrolyte suppressed the electrode disintegration and improved the cycling performance of the P-doped Si electrode. Raman mapping (Fig. 3a and b) was measured at a narrow area (7×7 μm^2). Thus, to investigate whether the above insights can be obtained in a wide area, the Raman spectra were measured at an arbitrary point of 100 μm^2. Fig. 3c shows the dependence of the mean value of the Raman shift of the P-doped Si and its standard deviation on the cycle number in the organic and ionic liquid electrolytes. Regardless of the electrolyte, the Raman shift decreased with an increase in the cycle number and reached a constant value after 2 cycles. Although the median was nearly the same, the standard deviation in the ionic liquid electrolyte was smaller than that in the organic electrolyte, which is a similar trend for the Si-alone electrode (Fig. S4). This result revealed that the alloying-dealloying reaction of P-doped Si with Li in the ionic liquid electrolyte was homogeneous and that the results of Fig. 3a and b can be reflected in the wide area.

Because not all ionic liquid electrolytes may improve the cycling performance of the P-doped Si electrode, we investigated the performance in various ionic liquid electrolytes, as shown in Fig. 4a.

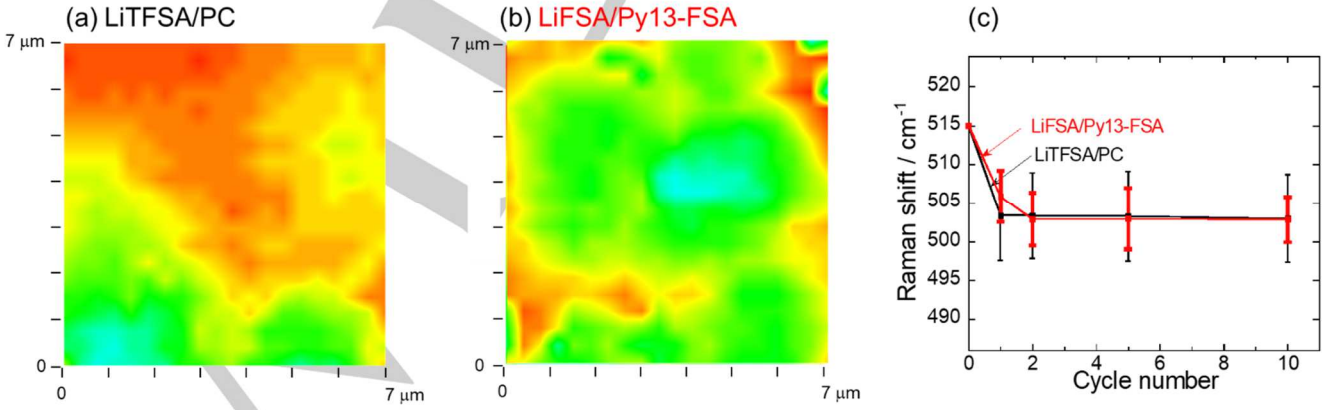

Figure 3. Raman images of the P-doped Si electrode surface after the 10th cycle in the electrolytes using (a) LiTFSA/PC and (b) LiFSA/Py13-FSA. The Raman map was made by plotting the band position with maximum intensity in the wavenumber range from 490 to 520 cm^{-1}. The mapping area is 7 × 7 μm^2. Red-colored regions indicates the presence of crystalline Si (unreacted Si with Li). (c) The correlation between the Raman shift and cycle number of P-doped Si electrodes. The charge/discharge tests were carried out in 1 M LiFSA/Py13-FSA or LiTFSA/PC.

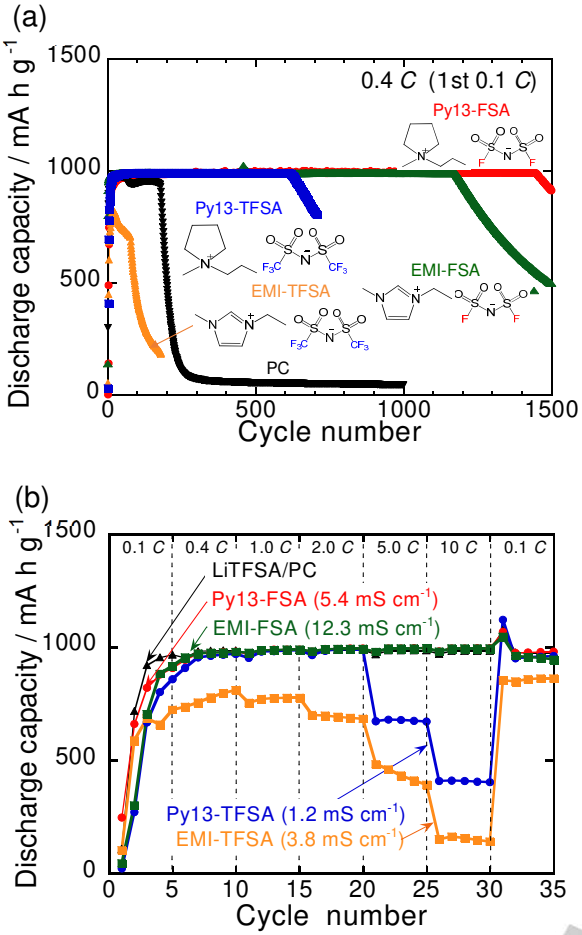

Figure 4. (a) Cycling performance and (b) rate capability of a P-doped Si electrode in various ionic liquid electrolytes.

We selected a pyrrolidinium-based ionic liquid electrolyte with excellent resistance against oxidation and reduction and an imidazolium-based electrolyte with a relatively high ionic conductivity [19,20]. Comparing two ionic liquid electrolytes consisting of the Py13 cation, the discharge capacity of 1000 mA h g^{-1} decayed at approximately 600 cycles in the TFSA-based electrolyte, whereas the P-doped Si electrode maintained the capacity over 1400 cycles in the FSA-based electrolyte. This difference should be due to a decomposition mechanism of anion species; the S-N bond of the TFSA anion is preferentially broken [21], whereas the S-F bond of the FSA anion is broken and F^- is released quickly, resulting in the formation of LiF. Since LiF contributes to the structural stability of the surface film [18], the P-doped Si electrode exhibited excellent cycling life in the FSA-based ionic liquid electrolyte. When the EMI cation was used, the discharge capacity of the P-doped Si electrode did not reach 1000 mA h g^{-1} and decayed at the early stage in the TFSA-based electrolyte, which is inferior to the performance in the organic electrolyte. This result is because the EMI cation has poor reduction resistance and is easily decomposed. Thus, the CE in EMI-TFSA was much lower than that in the other electrolytes (Fig. S5a). In contrast, the electrode maintained the capacity over 1200 cycles in the FSA-based electrolyte. This tendency of cycling performance is the same in an ionic liquid electrolyte consisting of a Py13 cation, which demonstrates that an FSA-based electrolyte is useful for improving the cycle life of a P-doped Si electrode.

Fig. 4b shows the rate performance of P-doped Si electrodes in various ionic liquid electrolytes. The electrode exhibited remarkable rate performance in the FSA-based electrolytes, which is comparable to the performance in organic electrolytes. The FSA-based ionic liquid electrolytes showed higher ionic conductivity than the TFSA-based electrolyte (LiFSA/Py13-FSA: 5.4 mS cm^{-1}, LiFSA/EMI-FSA: 12.3 mS cm^{-1}, LiTFSA/Py13-TFSA: 2.3 mS cm^{-1}, LiTFSA/EMI-TFSA: 3.8 mS cm^{-1}, LiTFSA/PC: 5.6 mS cm^{-1}). While the conductivity of LiTFSA/EMI-TFSA was higher than that of LiTFSA/Py13-TFSA, the rate capability was poorer in EMI-based electrolytes. As mentioned above, this result is attributed to the poor reduction resistance of the EMI cation (Fig. S5b). Thus, the P-doped Si electrode only showed poor rate capability; the discharge capacity did not reach 1000 mA h g^{-1} in LiTFSA/EMI-TFSA. Since the diffusion of Li^+ in the electrolyte is dominant at high rates, the electrode showed excellent rate performance in FSA-based electrolytes with high ionic conductivity. Therefore, for the P-doped Si electrode, it was revealed that both LiFSA/Py13-FSA and LiFSA/EMI-FSA can effectively realize the potential of the negative electrode performance. In addition, we confirmed that the electrode showed much more superior rate performance than the Si-alone electrode; a discharge capacity of 500 mA h g^{-1} was only retained at 10 *C* in LiFSA/Py13-FSA (data not shown).

In summary, we investigated the electrochemical performance of a P-doped Si negative electrode for a LIB in various liquid electrolytes. Although the P-doped Si electrode retained a discharge capacity of 1000 mA h g^{-1} only up to 170 cycles in an organic electrolyte, the electrode showed an excellent cycling performance with a capacity beyond 1200 cycles in the FSA-based ionic liquid electrolytes. The lithiation/delithiation reaction of P-doped Si occurred uniformly on the electrode in the ionic liquid electrolytes, and the expansion and contraction of P-doped Si occurred overall, which avoided high stress and large strain. Thus, the electrode disintegration was suppressed in the ionic liquid electrolytes. In addition, the cycling performance in FSA-based electrolytes was much more superior than that in TFSA-based electrolytes. LiF is more likely to form in FSA-based electrolytes. Since LiF contributes to the structural stability of the surface film, the P-doped Si electrode exhibited excellent cycle life in the electrolytes. In addition, the electrode showed good rate performance in FSA-based electrolytes, which resulted from higher ionic conductivity. It is concluded that FSA-based ionic liquid electrolytes could be successfully applied to a P-doped Si negative electrode and that they represent one type of promising electrolyte for next-generation LIBs with this electrode.

Supporting Information Summary

An experimental section, characterization data, cycling performance of the Si-alone electrode, and other electrochemical performance of the P-doped Si electrode are available in the Supporting Information.

Acknowledgements

This work was partially supported by the Japan Society for the Promotion of Science (JSPS) KAKENHI, grant numbers JP17H03128, JP17K17888, and JP16K05954.

Keywords: Electrochemistry • Gas deposition • Ionic liquid • Lithium ion battery • Phosphorus • Silicon

[1] M. N. Obrovac, L. Christensen, *Electrochem. Solid-State Lett.*, **2004**, *7*, A93–A96.
[2] T. D. Hatchard, J. R. Dahn, *J. Electrochem. Soc.*, **2004**, *151*, A838–A842.
[3] X. H. Liu, L. Zhong, S. Huang, S. X. Mao, T. Zhu, J. Y. Huang, *ACS Nano*, **2012**, *6*, 1522–1531.
[4] K. Zhao, M. Pharr, Q. Wan, W. L. Wang, E. Kaxiras, J. J. Vlassak, Z. Suo, *J. Electrochem. Soc.*, **2012**,*159*, A238–A243.
[5] N. Ding, J. Xu, Y. X. Yao, G. Wegner, X. Fang, C. H. Chen, I. Lieberwirth, *Solid State Ionics*, **2009**, *180*, 222–225.
[6] J. Xie, N. Imanishi, T. Zhang, A. Hirano, Y. Takeda, O. Yamamoto, *Mater. Chem. Phys.*, **2010**, *120*, 421–425.
[7] G. Zhao, Y. Meng, N. Zhang, K. Sun, *Mater. Lett.,* **2012**, *76*, 55–58.
[8] S. Rousselot, M. Gauthier, D. Mizouzi, B. Lestriez, D. Guyomard, L. Roue, *J. Power Sources*, **2012**, *202*, 262–268.
[9] P. Wang, Y. Zhang, Y. Yin, L. Fun, K. Sun, *ACS Appl. Mater. Interfaces*, **2018**, *10*, 11708–11714.
[10] Y. Domi, H. Usui, M. Shimizu, Y. Kakimoto, H. Sakaguchi, *ACS Appl. Mater. Interfaces*, **2016**, *8*, 7125–7132.
[11] H. Usui, Y. Yamamoto, K. Yoshiyama, T. Itoh, H. Sakaguchi, *J. Power Sources*, **2011**, *196*, 3911–3915.
[12] H. Usui, T. Masuda, H. Sakaguchi, *Chem. Lett.*, **2012**, *41*, 521–522.
[13] K. Yamaguchi, Y. Domi, H. Usui, H. Sakaguchi, *J. Power Sources*, **2017**, *338*, 103–107.
[14] K. Yamaguchi, Y. Domi, H. Usui, H. Sakaguchi, *ChemElectroChem*, **2017**, *4*, 3257–3263.
[15] M. Shimizu, H. Usui, K. Matsumoto, T. Nokami, T. Itoh, H. Sakaguchi, *J. Electrochem. Soc.*, **2014**, *161*, A1765–A1771.
[16] M. Shimizu, H. Usui, T. Suzumura, H. Sakaguchi, *J. Phys. Chem. C*, **2015**, *119*, 2975–2982.
[17] A. Tokranov, B. W. Sheldon, C. Li, S. Minne, X. Xiao, *ACS Appl. Mater. Interfaces*, **2014**, *6*, 6672–6686.
[18] D. M. Piper, T. Evans, K. Leung, T. Watkins, J. Olson, S. C. Kim, S. S. Han, V. Bhat, K. H. Oh, D. A. Buttry, S.-H. Lee, *Nat. Commun.,* **2015**, *6*, 6230.
[19] H. Sakaebe, H. Matsumoto, *Electrochem. Commun.*, **2003**, *5*, 594–598.
[20] H. Matsumoto, H. Sakaebe, K. Tatsumi, M. Kikuta, E. Ishiko, Mi. Kono, *J. Power Sources*, **2006**, *160*, 1308–1313.
[21] S. Xiong, K. Xie, E. Blomberg, P. Jacobsson, A. Matic, *J. Power Sources*, **2014**, *252*, 150–155.

Entry for the Table of Contents

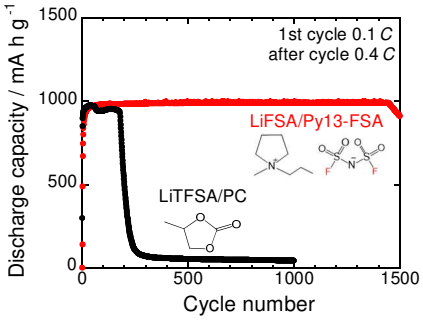

A P-doped Si electrode exhibited excellent cycling performance with a discharge capacity of 1000 mA h g^{-1} over 1400 cycles in an ionic liquid electrolyte, whereas the capacity decayed at approximately the 170th cycle in an organic electrolyte. It is concluded that the ionic liquid electrolytes could be successfully applied to a P-doped Si electrode and that they represent one type of promising electrolyte for next-generation LIBs with this electrode.